Available online at www.sciencedirect.com

ScienceDirect

Procedia Engineering 147 (2016) 478 – 483

Procedia Engineering

www.elsevier.com/locate/procedia

11th conference of the International Sports Engineering Association, ISEA 2016

Towards safer helmets: characterisation, modelling and monitoring

L. Andena[a,d*], F. Caimmi[a], L. Leonardi[a], A. Ghisi[b], S. Mariani[b,d], F. Braghin[c,d]

[a]*Dipartimento di Chimica, Materiali e Ingegneria Chimica, Politecnico di Milano, Piazza Leonardo da Vinci 32, 20133 Milano, Italy*

[b]*Dipartimento di Ingegneria Civile e Ambientale, Politecnico di Milano, Piazza Leonardo da Vinci 32, 20133 Milano, Italy*

[c]*Dipartimento di Meccanica, Politecnico di Milano, via La Masa 1, 20156 Milano, Italy*

[d] *E4Sport - Engineering for Sport Laboratory, Politecnico di Milano, Piazza Leonardo da Vinci 32, 20133 Milano, Italy*

Abstract

Bike and ski helmets are mainly made up of two layers: the external shell and the foam liner. The foam liner, typically made of expanded polystyrene (EPS) or polypropylene (EPP), is asked to provide energy absorption in case of impacts. Standard helmet design requires the foam to maximize this energy absorption, thus achieving large deformations (up to 25% in compression) while maintaining the stress level below a threshold value. To optimize the helmet construction in terms of foam composition, structure and density, reliable numerical models are required, which in turn need to be fed with accurate experimental data.

A characterisation of several foams was performed, including EPS and EPP having varying densities, under tensile and compressive stress states at varying strain rates. Typical mechanical parameters (elastic moduli and plateau stress in compression, Poisson's ratio) were compared with literature data and applicability of existing models to experimental results was discussed. A marked strain rate dependence – very important for impact applications – was accurately described using the Nagy phenomenological model. The foam microstructure was investigated using scanning electron microscopy (SEM) to assess structural changes before and after compression. The aforementioned mechanical features were then adopted in a rate-dependent constitutive law for crushable foams, to model the shock attenuation properties of helmets and validate the approach against available data.

Finally, a microelectromechanical system based in-helmet wireless micro monitoring system was developed and inserted in a helmet prototype. The system is capable of acquiring impact load spectra, providing valuable information to investigate generic impacts with varying angles and energy. In particular, it can monitor the effect of repeated micro-impacts on the residual energy absorption characteristics of the foam.

Peer-review under responsibility of the organizing committee of ISEA 2016

Keywords: traumatic brain injury (TBI); polymeric foams; numerical modelling; in-situ monitoring

1. Introduction

In recent years, sport injuries have attracted more and more interest, not only because of the short-term impact on athletes' performance but also because of the costs of possibly long rehabilitation periods and difficulties to fully recover. One striking example in this sense is represented by the Head Health Initiative of National Football League [1].

Focusing on traumatic brain injuries (TBIs) only, the Centre for Disease Control and Prevention (CPSC) estimated that around 450,000 sports-related head injuries were treated in U.S. hospital emergency rooms in 2009 [2]. Among the most impressive data is that children in the range of 10 to 14 years old show the highest rate of emergency visits associated with such sports-related TBIs. The actual incidence of head injuries may be potentially higher, as not-severe cases are typically self-treated. In Italy, a survey conducted by the Istituto Superiore di Sanità also revealed that every year around 30,000 accidents occur in ski areas, of which 25% involve underage children and 10% lead to mild TBIs [3].

In case of impacts, helmets have to prevent or reduce the outcome of mild TBIs thanks to a kind of cushioning effect, mainly linked to the mechanical behavior of their inner liner. The level of the impact-induced acceleration hitting the athlete brain is reduced by mechanisms of energy dissipation occurring while the mentioned liner deforms and possibly locally fails.

* Corresponding author. Tel.: +390223993289; fax: +390223993280.
E-mail address: luca.andena@polimi.it

Peer-review under responsibility of the organizing committee of ISEA 2016
doi:10.1016/j.proeng.2016.06.224

Accordingly, international standards like [4-6] provide requirements for the shock absorbing capacity in terms of acceleration peaks in the range of 250-300 g (g being the gravity acceleration) depending on country and sport, all measured in case of (guided) falls of headforms wearing the protective helmet. Not much care is usually devoted to the impact duration and to rotational accelerations, which were instead highlighted as further important parameters to classify the severity of the impact in, e.g. [7-8].

In this work, the focus is on bike and ski helmets that are basically made of a hard outer shell of polycarbonate, and a soft inner liner of polymeric foam, typically expanded polystyrene. With the goal of either enhancing the protection level, or reducing size and weight of the helmet to improve the athlete's comfort at the same safety level, the study was developed following three main research lines. First of all, tensile and compressive properties of polymeric foams were characterized in relation to their density and strain rate, the foam being the helmet constituent which is mainly responsible for cushioning. These data then allowed finite element numerical modelling of the whole helmet to be performed in order to describe its response to impacts. In parallel, a novel monitoring system based on microelectromechanical systems (MEMS) was designed and realized to perform measurements on existing helmets and new prototypes.

2. Characterisation

2.1. Experimental

Expanded Poly-Propylene (EPP) and Expanded Poly-Styrene (EPS) foams with varying relative densities were considered; materials nominal densities are reported in Table 1. These foams were produced from pre-expanded beads which were subsequently moulded into sheets/blocks.

Table 1. Materials.

Material	Expanded polystyrene				Expanded polypropylene							
Density [kg/m^3]	10	13	19	25	20	35	55	60	75	90	110	120
(Relative density [-])	(0.01)	(0.013)	(0.019)	(0.025)	(0.022)	(0.039)	(0.061)	(0.067)	(0.083)	(0.100)	(0.122)	(0.133)

Uni-axial compression and tensile tests were run on screw-driven dynamometer under crosshead displacement control conditions. All the tests were performed at 23°C temperature and 50% relative humidity. Five samples per density were tested.

EPS compression specimens were cut having nominal dimension of 40x40x40 mm, while EPP samples nominal dimensions were 13x13x13 mm. Strain rate dependence was investigated at three nominal values: 3×10^{-3}, 3×10^{-2} and 3×10^{-1} s^{-1}. A 10MPixel camera was used for the measurement of Poisson's ratio in compression.

Tensile tests were performed on dumbbell specimens having gauge length of 70 mm, width of 13 mm and thickness of about 12 mm; a fixed strain rate of 3×10^{-3} s^{-}1was adopted. Axial strain was measured with a Trio VE5000 video-extensometer.

To investigate foam morphology, samples were broken by bending a notched bar immersed in liquid nitrogen. Fracture surface were then metallized with palladium for scanning electron microscopy (SEM) observation.

2.2. Results

A good repeatability was observed in both tensile and compression tests, with exception of EPP compressive elastic modulus data, which presented a particularly high scatter. Poisson's ratio in compression was measured to be zero within experimental accuracy for EPP and EPS foams up to 0.6 strain.

The foam compression behaviour is consistent with the expected behaviour: a linear elastic region was followed by a collapse plateau and a final densification. Elastic moduli were evaluated in the initial region and plateau stresses were defined at 0.25 strain. In Fig. 1. mechanical properties are plotted against density and compared to the predictions from Ashby's model [9], which are given in Eq.s (1-2):

$$\frac{E^*}{E_S} \approx \Phi^2 \cdot \left(\frac{\rho^*}{\rho_S}\right)^2 + (1-\Phi)\cdot\frac{\rho^*}{\rho_S} + \left(\frac{p_0}{E_S}\right)\cdot\frac{(1-2\cdot\nu^*)}{\left(1-\rho^*/\rho_S\right)} \tag{1}$$

$$\frac{\sigma^*_{pl}}{\sigma_y} \approx 0.3\cdot\left(\Phi\cdot\frac{\rho^*}{\rho_S}\right)^{3/2} + 0.4\cdot(1-\Phi)\cdot\frac{\rho^*}{\rho_S} + \left(\frac{p_0 - p_{at}}{\sigma_y}\right) \tag{2}$$

where E^* is the foam modulus; E_S stands for the solid material elastic modulus; Φ is the volume fraction of solid in the edges; ρ^* is the foam nominal density; ρ_s is the base material density; p_0 is the pressure inside the cells; ν^* is the foam Poisson's coefficient; σ^*_{pl} is the plateau stress; σ_y is the solid material yield stress and p_{at} is the atmospheric pressure.

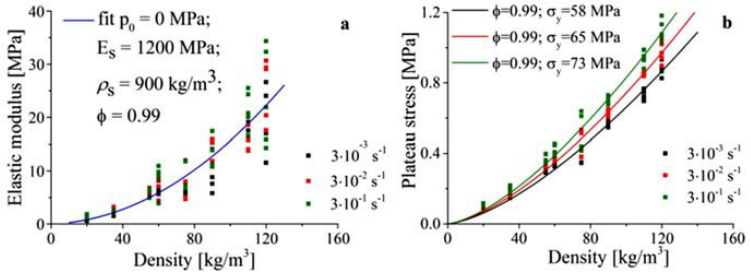

Fig. 1. (a) EPP compressive modulus data collected at three strain rates and fitted to Eq. (1) (blue line), using material parameters indicated in the legend; (b) EPP plateau stress data fitted to Eq. (2) for each strain rate using the model parameters indicated in the legend.

In the fitting procedure for $E^*$and σ^*_{pl}, these base material density and modulus were used: $\rho_{s,PP}$ = 900 kg/m^3, $\rho_{s,PS}$ = 1050 kg/m^3, $E_{s,PP}$ = 1200 MPa, $E_{s,PS}$ = 3200 MPa. The value of Φ was obtained from the modulus fit. Plateau stress was fitted using these Φ values and base material yield stresses were obtained. Internal air pressure p_0 was considered negligible. In Figs. 2-3., average values are reported together with standard deviation indicated by error bars.

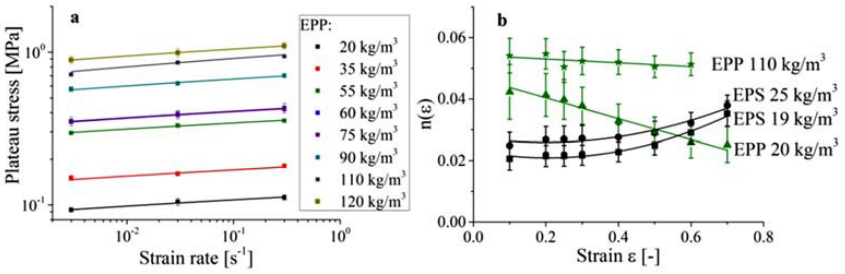

Fig. 2. (a) EPP foams plateau stresses vs. strain rate; (b) Nagy's model index vs. strain and fits for EPS (19 and 25 kg/m^3) and EPP (20 and 110 kg/m^3).

Moduli do not depend significantly on strain rate while for plateau stresses a dependence on strain rate was observed as shown in Fig. 2.(a). Because of this, Nagy's phenomenological model [10], given in Eq. (3), was fit to the experimental data. Accordingly, the stress $\sigma(\varepsilon)$ at a given strain rate $\dot{\varepsilon}$ is related to the stress $\sigma_0(\varepsilon)$ at a reference one $\dot{\varepsilon}_0$ through the strain dependent index $n(\varepsilon)$.

$$\sigma(\varepsilon) = \sigma_0(\varepsilon) \cdot \left(\frac{\dot{\varepsilon}}{\dot{\varepsilon}_0} \right)^{n(\varepsilon)} \tag{3}$$

For EPP, Nagy's power index depends linearly on strain (for relatively dense materials a very little dependence, if any, is observed), while for EPS a quadratic dependence on strain was observed for all samples, as can be seen in Fig. 2.(b).

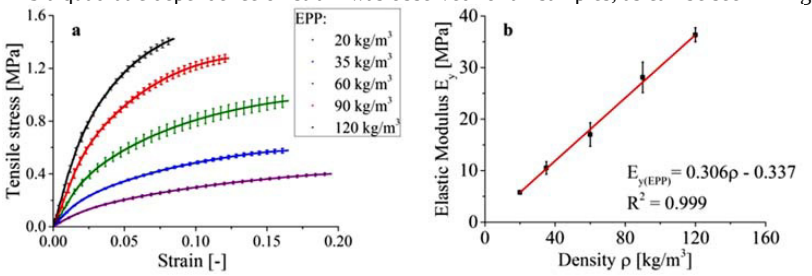

Fig. 3. (a) Tensile behaviour of five EPP foams having nominal densities reported in the legend; (b) tensile elastic modulus vs. foam density fitted by the linear equation reported in the figure and drawn in red in the graph.

The tensile behaviour was found to be strongly non-linear, as shown in Fig. 3 for EPP samples of varying density. The elastic modulus was determined approximating the region up to 0.02 strain as linear. A linear relationship was found for modulus vs.

density dependence. Tensile moduli of both EPS and EPP were higher than compressive ones and moduli mismatch decreased going towards higher densities.

To get information on the foam structure from the SEM images, after adjusting contrast and sharpness, the cellular wall structure was approximated with 2D polygons. From SEM images taken after compression we noted that wrinkles appeared on cell walls and were visible even if the foam recovered entirely the deformation applied. At densities higher than 60 kg/m^3 foam recovery did not take place and cell walls remained in the deformed configuration with folded cell walls, as can be seen in Fig. 4.

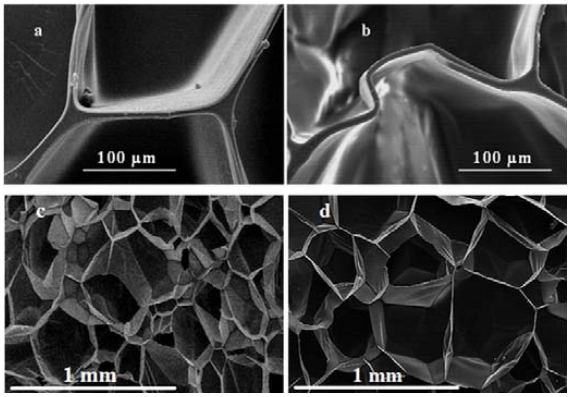

Fig. 4. (a) as received EPP 120 kg/m^3 foam; (b) folded cell wall belonging to an EPP 120 kg/m^3 foam (after compression); (c) as received EPP 20 kg/m^3 foam; (d) EPP 20 kg/m^3 after compression.

3. Numerical modelling

The experimental data were used to calibrate a constitutive law able to capture the nonlinear response of the foam material at varying strain rates, which is essential to describe the helmet's shock absorbing capabilities. With the aim to build a model useful for a structural analysis of helmets where the foam is the main constituent, we adopted the crushable foam model developed by Deshpande and Fleck [11] for metallic foams and already implemented in a commercial code [12]. As far as compression loading is considered, the model provides isotropic elasticity followed by a plastic evolution featuring volumetric hardening beyond the compression yield stress σ_c^0. Therefore, the model actually represents a phenomenological interpretation of material behavior, acceptable during the loading conditions considered. A further approximation has been applied in the tensile region, where i) the Young's modulus has been considered coincident with the compression value, and ii) the yield surface almost does not evolve at difference with the aforementioned compression region. This behaviour has been graphically depicted in Fig. 5 in the meridian stress plane (combining deviatoric and hydrostatic stress), where the main parameters adopted for the model have been also indicated. Relevant material parameters obtained from experimental tests were extrapolated to the desired strain rate(s) using Nagy's model. As an example, the values considered for the 120 kg/m^3 EPP foam are collected in Table 2; they were used in the numerical simulation shown in the following.

σ_c^0 [MPa]	$k = \sigma_c^0/p_c^0$	$k_t = p_t/p_c^0$
0.7017	0.6	2.0

Table 2. Material parameters for EPP 120 kg/m^3 foam (for symbol definition see Fig. 5).

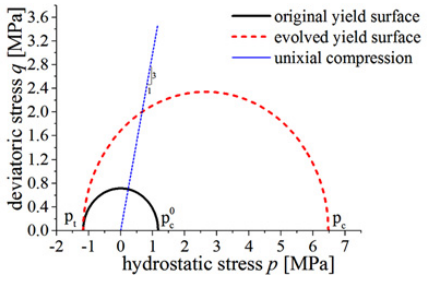

Fig. 5. Original and evolving yield surface used for EPP 120 kg/m^3 foam.

A ski helmet under a typical impact test has been analysed as an example: a metal headform (not represented here) has been placed inside the helmet and a steel impactor has been directed towards the external polycarbonate shell (again, not shown in the following picture) at a relative velocity of 5.425 m/s, corresponding to a theoretical free fall from 1.5 m. Coulombian contact has been considered between each of the parts constituting the system, in particular between the steel impactor and the outer shell, between the regions of the shell not jointed to the foam and the foam part itself (the latter shown in Fig. 6.(b)), and between foam and headform. Since the geometry and the materials for the impactor and the headform are standardized (e.g. [4], [13]), the friction coefficients can be estimated within reasonable accuracy for the analysis; however, for actual impacts with different kind of contact surfaces a study of the effects of varying friction is advisable.

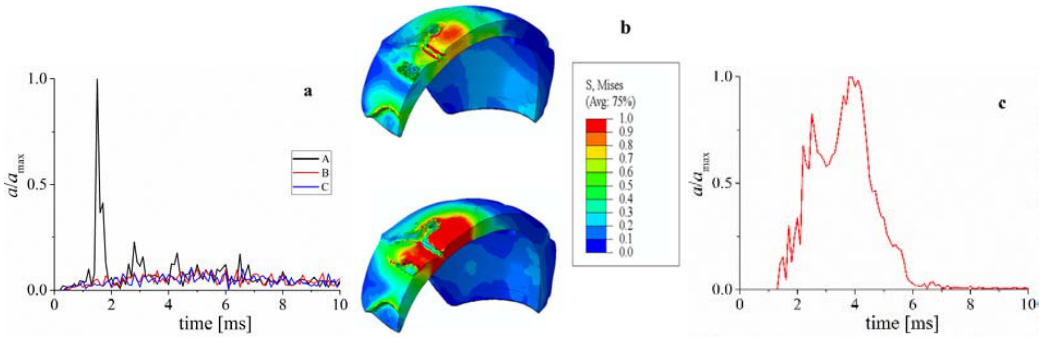

Fig. 6. Simulation of impact test: (a) outcomes in terms of relative acceleration at selected points at the interface between foam and headform, (b) von Mises stresses (normalized to the maximum value) inside the foam at t=1.4 ms (upper) and t=3.4 ms (lower), (c) normalized acceleration at the centre of the headform.

By recording the acceleration signals during the 10 ms-long impact observation time at selected points (Fig 6.(a)) and evaluating the corresponding stress state in the foam (only half of the foam in the helmet has been represented in Fig. 6.(b)), it was possible to gain insights on the best locations where to place the in-situ monitoring sensors, depending on the impact direction. Besides these numerical data, the outcome in terms of acceleration signals inside the headform (Fig. 6.(c)) was also collected for comparison with the experiments.

4. Monitoring

With the aim of evaluating helmets' performance in terms of kinetic energy absorption during impacts, a distributed acquisition system was designed and realized. The adoption of this kind of system, instead of a single accelerometer as prescribed in the standards, allows obtaining more information useful to evaluate the helmet's response in different areas and facilitate safety improvements.

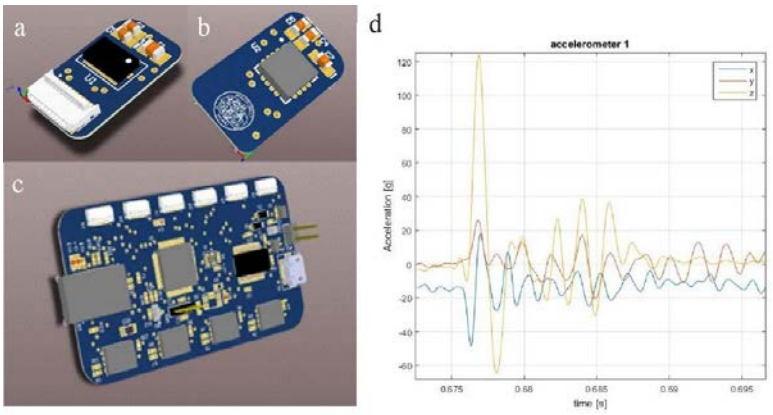

Fig. 7. MiniIMU: (a) Top view; (b) Bottom view; (c) Data acquisition board; (d) output recorded by the 3-axis accelerometer after a shock.

This system comprises up to six IMUs, placed inside the helmet, and a miniaturized acquisition board, fixed at the back of the helmet, that is able to both acquire data from the inertial sensors and send these data to a PC through a wireless connection. Since the inertial measurement units have to be placed inside the helmet, their dimensions were minimized as shown in Fig. 7.(a-c). On

these *miniIMUs* a 3-axis digital MEMS gyroscope and a 3-axis digital MEMS accelerometer are mounted, while the connection with the acquisition board is ensured by a very thin (1mm in height) FPC connector and an FFC cable. The overall dimensions of the board are 14mm x 8mm x 2.6mm. For what concerns the 3-axis MEMS accelerometer, the ADXL375 accelerometer by Analog Devices was selected due to its full-scale range of ± 200g, its high output data-rate (3200Hz) and bandwidth, as well as some functions like the internal FIFO buffer and the shock detection ability that ensure a more easy and effective management of sensors' incoming and outgoing dataflow. Instead, for what concerns the 3-axis MEMS gyroscope, the MAX21000 gyroscope by Maxim Integrated was chosen for his high signal to noise ratio, high and selectable output data-rate, configurable full-scale range up to 2000dps and highly customizable low and high pass filters. The sensors' management and the incoming data processing are carried out by the developed acquisition board. This device is mainly composed by: a 16-bit DSP microcontroller, that manages the sensors, the peripherals and the incoming and outgoing data flow; four 64Mbit Flash memories that allow recording the data retrieved from the IMUs; a Bluetooth transceiver; an USB transceiver to communicate with a remote PC. The power needed to operate the board is supplied by a mini LiPo battery that can be charged simply connecting the board with a micro-USB cable, as the charger is embedded onboard.

The acquisition loop is the following: once powered, the device scans which IMUs are connected and initializes the sensors and peripherals; then, it waits until the *start* command is issued from the remote PC to begin data acquisition and recording that ends when the remote PC sends a *stop* command or when onboard memories are full. The acquired data are then retrieved from memories and sent to the remote PC. Through a dedicated software that runs on the remote PC, all these operations are straight forward and the user is able to easily interact with the device in order to manage the acquisition system (start and stop the acquisition, change parameters, erase the memories and so on), and retrieve the acquired data. Fig. 7.(d) shows an example of the typical output given by the system after a shock applied to a helmet prototype.

Discussion and Conclusions

This work presents a three-step approach to improve the helmets' construction. A first, essential step is a correct representation of the mechanical behavior of the foam constituent materials, which are mainly responsible for the shock absorption characteristics of the helmets. A large set of data was obtained and existing models have been used to describe the effects of both density and rate; some variations in deformation mechanisms however suggest that changes in the foam structure can play a role, too. Subsequently, these data was used to calibrate a numerical model which – based on the small scale laboratory tests – can predict the response of an helmet undergoing an impact test. Within the model, parameters such as the foam type or its spatial density distribution can be easily altered to highlight their effect on the resulting accelerations which are transferred to the head, for any given impact condition (e.g. in terms of speed, energy or direction). Once a suitable objective function is defined, the numerical model can be exploited to optimize the helmets construction, improving the users' safety. A numerical optimization procedure is currently being developed. In parallel, an advanced monitoring system has already been created and tested. A distributed monitoring system is the third key step for the validation of the numerical model's predictions, allowing to process a much greater volume of information compared to single-accelerometer configurations currently used in helmets' testing.

Acknowledgements

This work was supported by Fondazione Cariplo – project "Safer Helmets" and Politecnico di Milano – Advanced Manufacturing Laboratory.

References

[1] NFLGEbrainchallenge.com, accessed on 14 January 2016.
[2] http://www.cdc.gov/features/Concussion/, accessed on 14 January 2016.
[3] Giustini M, Fondi G, Pitidis A, Cedri C, Crenca A, Taggi F. *Il sistema SIMON per la sorveglianza degli incidenti in montagna (2003-2006)*. Istituto Superiore di Sanità, Rapporti ISTISAN 07/1; in Italian; 2007.
[4] EN 1077. *Helmets for alpine skiers and snowboarders;* 2007.
[5] EN 1078. *Helmets for pedal cyclists and for users of skateboards and roller skates*; 2012.
[6] ASTM F1045. *Standard Performance Specification for Ice Hockey Helmets*; 2015.
[7] Wilcox B et al. Head impact exposure in male and female collegiate ice hockey players. J Biomech 2014;47:109–114.
[8] Greenwald RM, Gwin JT, Chu JJ, Crisco JJ. Head Impact Severity Measures for Evaluating Mild Traumatic Brain Injury Risk Exposure. Neurosurg 2008;62:789-798.
[9] Gibson LJ, Ashby MF. *Cellular Solids Structure and Properties*, Cambridge University Press, Cambridge (UK); 2008.
[10] Nagy A, Ko WL, Lindholm US. Mechanical Behavior of Foamed Materials under Dynamic Compression. J Cell Plast 1974; 10:127-134.
[11] Deshpande VS, Fleck NA. Isotropic constitutive models for metallic foams. J Mech Phys Solids 2000; 48:1253-1283.
[12] ABAQUS Documentation, release 14. Dassault Systèmes, Providence, RI, USA.
[13] BS EN 960. Headforms for use in the testing of protective helmets, 2006.